Joint Pathology Center
Veterinary Pathology Services

WEDNESDAY SLIDE CONFERENCE 2025-2026

Conference #10 5 November 2025

CASE I:

Signalment:
8-year-old female spayed wire-haired terrier (*Canis familiaris*)

History:
The dog had history of acute glaucoma with bullous retinal detachment, kidney disease, and recent seizures. This animal was treated with fortekor and diethylstilbestrol.

Gross Pathology:
The dog had moderate amounts of body fat stores and normal muscle mass. The thoracic cavity contained approximately 40 ml of red-tinged, watery fluid. The lungs were mottled dark and bright red, heavy, wet, and non-collapsed; abundant pink foamy fluid oozed from the cut surface. The heart was rounded; the left ventricular free wall was 22 mm thick, and the right ventricular free wall was 5 mm thick (left ventricular hypertrophy). The left atrium was mildly dilated. The leaflets of the mitral valve were shrunken, thickened, and nodular (myxomatous valvular degeneration or endocardiosis). The right ventricle had multifocal, slightly raised, areas of subendocardial hemorrhage. In the abdominal cavity, the stomach contained moderate amounts of clear mucoid material. The intestinal tract showed multifocal areas of mucosal congestion. The pancreas had a diffuse nodular surface (nodular hyperplasia). The spleen had multifocal, small, dark-red nodules scattered throughout the surface.

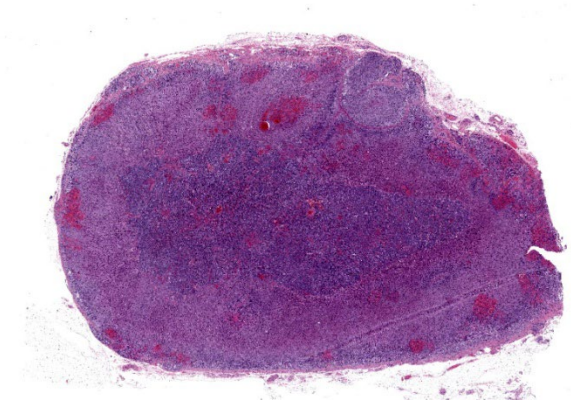

Figure 1-1: Adrenal gland, dog. One section of adrenal gland is submitted for examination. There is a focal cortical nodule and intracapsular hyperplasia of zona-glomerulosa cells. There is multifocal hemorrhage randomly scattered throughout the cortex and medulla.. (HE, 10X)

Multifocal areas of mucosal hemorrhage were noted in the trigone of the urinary bladder. The brain showed multifocal areas of meningeal hemorrhage over the occipital lobes. No gross abnormalities were observed in the rest of the carcass.

Laboratory Results:
N/A

Microscopic Description:
Adrenal glands: Multifocally, the small arteries and arterioles within the cortex and medulla show marked thickening of their walls, and narrowing or obliteration of their lumen, by intramural deposition of plasma proteins (consistent with hyaline arteriolosclerosis).

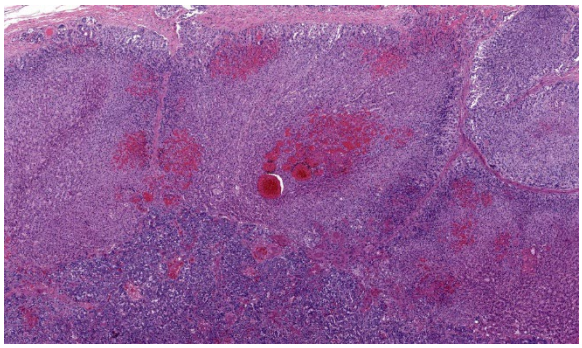

Figure 1-2: Adrenal gland, dog. There are numerous areas of sinusoidal congestion and hemorrhage scattered throughout the cortex and medulla. (HE, 52X)

Some vessels show intramural laminar deposits of plasma proteins (onion-skinning). Many sinusoidal vessels in the medulla are occluded by fibrin thrombi and are frequently effaced by hyaline material.

Contributor's Morphologic Diagnoses:
Adrenal glands: Multifocal hyaline arteriolosclerosis.
Condition: Hypertensive vasculopathy.
Other diagnoses (tissues not included in the submission):
Kidneys: Glomerulonephritis, diffuse, global, severe, subacute to chronic.
Eye globes: Bilateral retinal detachment with hyaline arteriolosclerosis, subretinal hemorrhage, and retinal atrophy (secondary glaucoma).
Heart, brain (choroid plexus), and spleen: Multifocal hyaline arteriolosclerosis.
Heart, right ventricle: Myocardial infarction, multifocal, acute.
Heart, mitral valve: Myxomatous valvular degeneration (endocardiosis).
Heart: Left ventricular hypertrophy.
Stomach: Mucosal necrosis and mineralization (uremic gastropathy).

Contributor's Comment:
Arteriolosclerosis is defined as "hardening of small arterial vessels" and consists of a group of arteriolar lesions often characterized as either predominantly hyaline or predominantly hyperplastic.[4] Hyaline degeneration (intimal hyalinosis), such as that seen in this case, refers to the histologic observation of amorphous, brightly eosinophilic material in vessel walls. This material stains magenta with periodic acid-Shiff (PAS) and often appears glassy.[4,5] It is a common vascular lesion resulting from accumulation of various serum plasma components in the subendothelial space and often extends into the media.[5] This lesion can be seen in various conditions, such as hypertension, diabetes mellitus, and focal segmental glomerulosclerosis (FSGS).[5] Thickening of the arteriolar wall due to accumulation of plasma proteins may lead to luminal narrowing and local ischemia.[4]

In humans, the most common inciting cause is hypertension. The pathogenesis in domestic animals is often not confirmed; most of the postmortem findings in the present case were consistent with systemic hypertension secondary to renal disease.[4] Although both primary and secondary hypertension have been reported in dogs, the latter is more common.[4]

Renal disease, such as in this case, is likely the most common cause of hypertension in dogs; however, since renal disease can be both the cause and consequence of systemic hypertension, it can be challenging to discern whether hypertensive vascular lesions are the result of primary or secondary hypertension.[4] Primary hypertensive lesions can lead to renal hypoperfusion, which activates the renin-angiotensin-aldosterone system, leading to more hypertension.[4] On the other hand, chronic renal disease often results in unbalanced excretion/retention of sodium and water, which

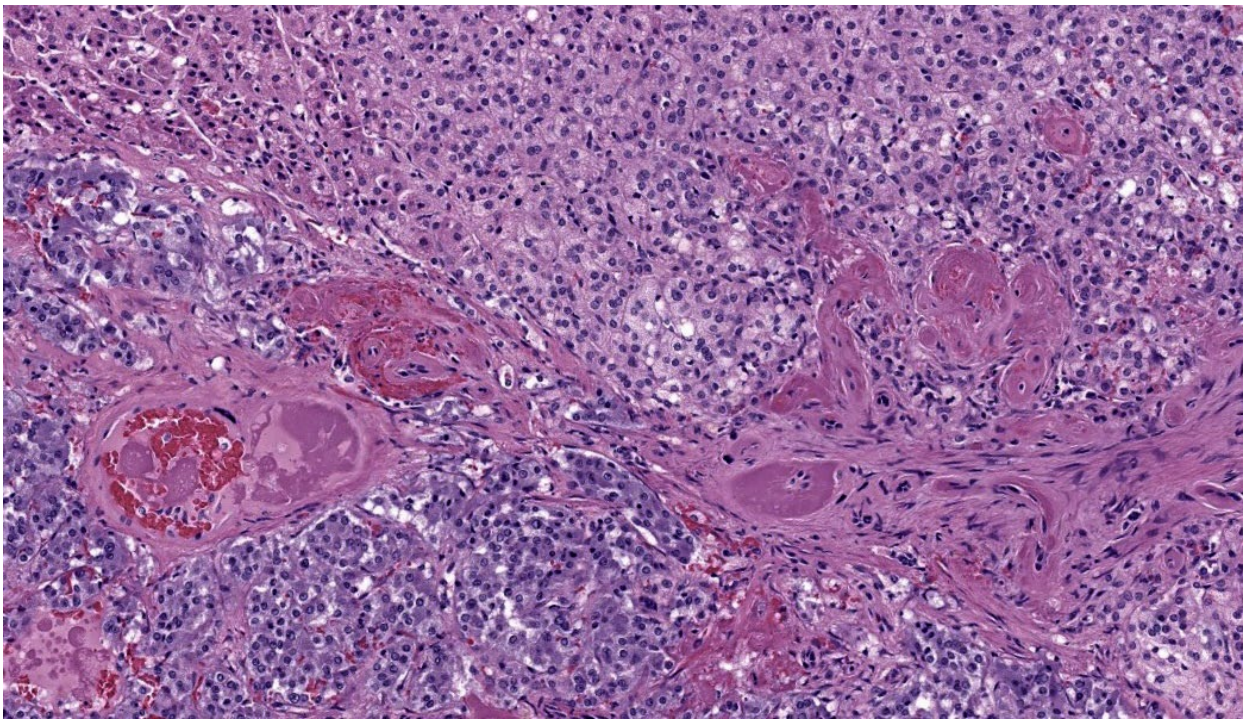

Figure 1-3: Adrenal gland, dog. Throughout the section (here at the corticomedullary junction), arteriolar profiles are tortuous, and the walls of arterioles are expanded by an accumulation of protein which expands the wall, effaces the tunica intima and smooth muscle cells, and compromises the lumen. There is periarteriolar hemorrhage. (HE, 261X)

leads to blood volume expansion and secondary hypertension.[4] Regardless of the initial inciting cause, hypertension becomes self-perpetuating as medial hypertrophy and hyalinization of arteries lead to hypoperfusion of organs, such as the kidney, and promotes additional hypertension and vascular damage.[4] Other lesions associated with secondary hypertension include hypertensive retinopathy with retinal detachment and left ventricular hypertrophy, which were also seen in this case.

Contributing Institution:
Veterinary Pathology – Western College of Veterinary Medicine
(https://wcvm.usask.ca/departments/vet-pathology.php)

JPC Diagnoses:
Adrenal gland, arterioles: Fibrinoid necrosis, chronic, diffuse, moderate, with fibrin thrombi and hemorrhage.

JPC Comment:
Conference 10 was moderated by the steadfast former Training Officer (and former WSC Coordinator) of the JPC, LTC Sarah Cudd! She chose to focus her conference cases on board-worthy entities and critical concept discussions for residents. This first case was challenging for participants and served as an excellent segway into a review of hypertension and atherosclerosis.

Discussion began with the differences between arteriosclerosis and atherosclerosis. Arteriosclerosis, meaning "hardening of arter-

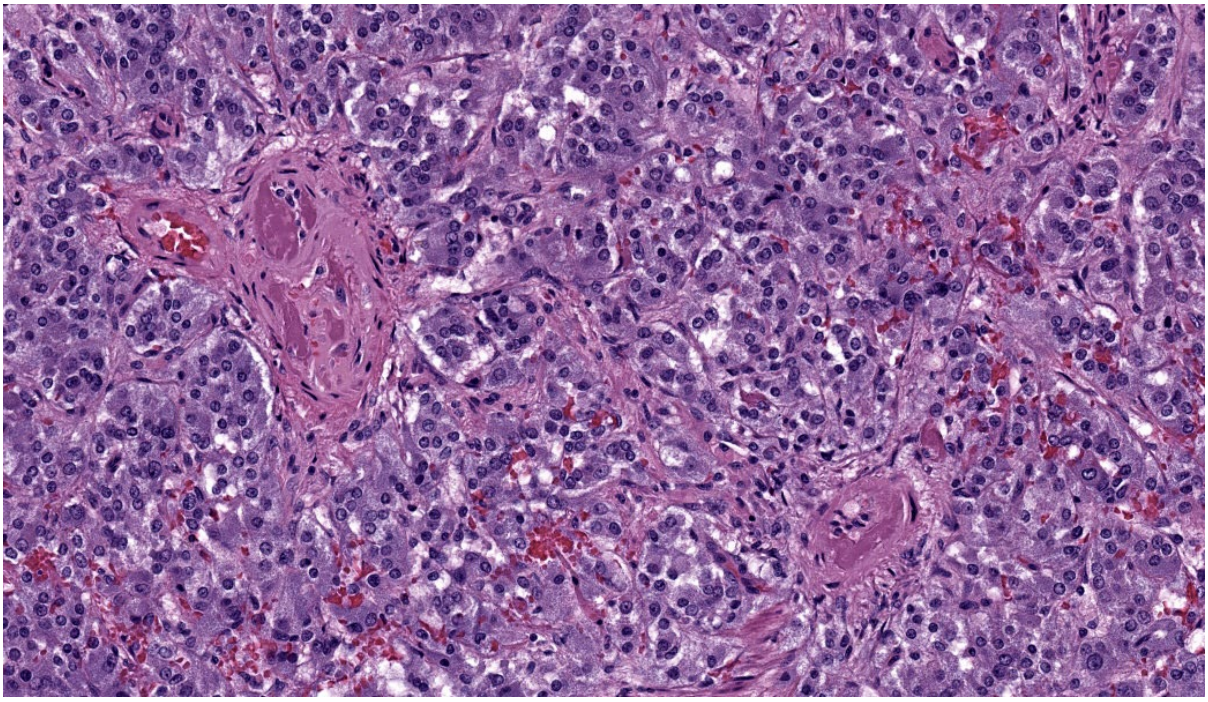

Figure 1-4: Adrenal gland, dog. Affected arterioles often contain fibrin thrombi. (HE, 451X)

ies", is characterized as a proliferative and degenerative arterial change in the absence of inflammation with thickening of the tunicas media and intima. Smooth muscle cells from the tunica media migrate to the tunica intima under the influence of platelet-derived growth factor PDGF), which stimulates smooth muscle cell migration and growth by binding to its receptors on the muscle cell surface. This triggers a series of internal signaling pathways that promote cell proliferation and migration, such as the PI3K/Akt/mTOR cascade. This pathway ultimately activates transcription factors that cause changes in gene expression and cell cycle progression via the activation of receptor tyrosine kinases. Atherosclerosis, on the other hand, is a subset of arteriosclerosis and is characterized histologically by degenerative fatty changes with cholesterol clefts, foam cells (which can be either macrophages or smooth muscle cells), and extra cellular lipid within arterial walls. Atherosclerosis is the most common type of arteriosclerosis in humans and is rarely seen in dogs except in cases of hypothyroidism or diabetes mellitus that contribute to hyperlipidemia. Miniature Schnauzers are genetically predisposed to atherosclerosis due to idiopathic hyperlipoproteinemia. Watanabe rabbits are also predisposed to and used as a research model for atherosclerosis due to a genetic mutation in their LDL receptors.

So, what about arteriolosclerosis? How does that compare to arteriosclerosis? Arteriosclerosis usually affects large arteries, such as the abdominal aorta in horses, ruminants, and carnivores, and is an aging change. Arteriolosclerosis affects small arterioles and is largely due to endothelial damage secondary to hypertension. There are two types of arteriolosclerosis: hyaline and hyperplastic. The hyaline form is considered the acute stage. In the hyperplastic form, proliferation of smooth muscle cells

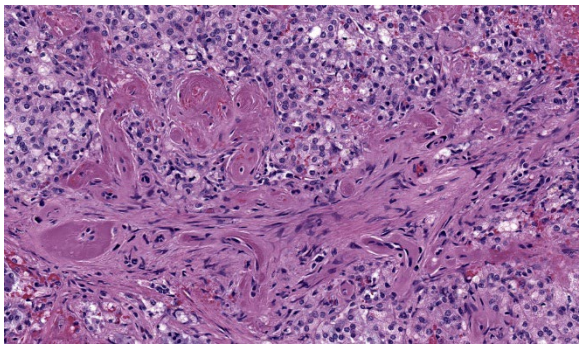

Figure 1-5: Adrenal gland, dog. Effete arterioles are surrounded by abundant fibroblasts and mature collagen, often giving cross sections of arterioles an "onion-skinned" appearance. (HE, 381X)

within the tunica intima, coupled with concentric fibrosis, can lead to a characteristic "onion-skinning" appearance of the affected vessels with chronicity.

Wrapping up conference discussion was a review of primary vs. secondary hypertension, which the contributor did an excellent job of covering in their comment. Hypertension causes hyaline arteriolosclerosis by causing endothelial damage, which then forces serum proteins from the blood out into the arteriolar walls where they accumulate and form deposits. This is traditionally referred to as "fibrinoid necrosis", and conference participants elected to use this term for the morphologic diagnosis. Additionally, the damage to the vessel walls from the increased pressure causes them to become tortuous and stimulates them to thicken and harden via smooth muscle proliferation and fibrosis as previously mentioned, reducing their elasticity and narrowing the lumen. This impairs blood flow and may result in thrombosis.[3] In cases of hypertension, the most common presenting clinical sign in affected animals is acute blindness secondary to hypertensive retinopathy.

With renal disease being one of the key drivers of hypertension in many species, a quick review of this pathogenesis is warranted. Renal disease causes secondary hypertension primarily through fluid retention. Injured kidneys are less able to remove excess fluid and sodium, which leads to an increased blood volume and, subsequently, an increased blood pressure. In primary hypertension leading to renal hypoperfusion, there is activation of the renin-angiotensin-aldosterone system (RAAS), which unfortunately only exacerbates the problem.

The RAAS first came under study in 1898 with the discovery of renin by Drs. Tigerstedt and Bergman when they found that renal extracts produced a vasopressor effect on tissue.[1] It wasn't until many years later that angiotensin and aldosterone were discovered and described, ultimately resulting in the RAAS we understand today.[1] RAAS becomes activated following an initial drop in blood pressure, during which less sodium is flowing through the kidneys.[1,2,3] The macula densa cells within the juxtaglomerular apparatus of

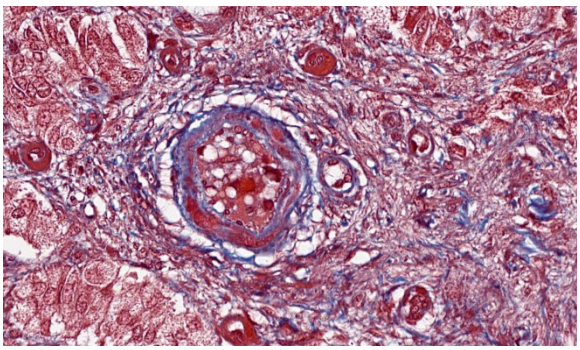

Figure 1-6: Adrenal gland, dog. A Masson's trichrome demonstrates the presence of mural collagen as well as protein deposits within the wall of affected arterioles. (Masson's trichrome, 581X).

the kidneys detect lower sodium levels within the proximal convoluted tubules and subsequently release prostaglandin E2 (PGE2).[2]

PGE2 then acts on juxtaglomerular cells within the afferent arterioles of the kidneys and causes them to release renin. From there, renin stimulates conversion of liver-produced angiotensinogen in the blood to angiotensin I within the kidneys.[2] Angiotensin-converting enzyme (ACE) then converts angiotensin I to active angiotensin II, which is a potent vasoconstrictor. Constriction of blood vessels subsequently stimulates the adrenal cortices to synthesize and release aldosterone, which then signals the kidneys to retain water and sodium from the distal convoluted tubules and collecting ducts, thereby increasing both blood volume and blood pressure.[2,3]

Angiotensin II also stimulates secretion of antidiuretic hormone (ADH) from the posterior pituitary, which increases the glomerular filtration rate by increasing water resorption from the kidneys.[2] It does this via the insertion of aquaporin-2 channels in the collecting duct.[2,3] It's not difficult to see from here how activation of RAAS makes a hypertensive problem worse. When coupled with a chronic arteriolosclerosis, it has been suggested that autoregulation of these systems becomes even further impaired and may result in additional increased systemic pressure to the glomerulus, further perpetuating renal disease and contributing to the vicious cycle of hypertension.[2]

References:

1. Basso N, Terragno NA. History about the discovery of the renin-angiotensin system. *Hypertension*. 2001;38(6):1246-9.
2. Manrique C, Lastra G, Gardner M, Sowers JR. The renin angiotensin aldosterone system in hypertension: roles of insulin resistance and oxidative stress. *Med Clin North Am*. 2009;93(3):569-82.
3. Nair R, Vaqar S. Renovascular Hypertension. [Updated 2023 May 22]. In: StatPearls [Internet]. Treasure Island (FL): StatPearls Publishing; 2025.
4. Robinson WF, Robinson NA. Cardiovascular system. In: Maxie MG, ed. Jubb, Kennedy, and Palmer's Pathology of Domestic Animals. Vol 3. – 6th ed. Philadelphia, PA: Elsevier; 2016: 59-60.
5. Olson JL. Hyaline arteriolosclerosis: New meaning for an old lesion. *Kidney International*. 2009;63:1162–1163.

CASE II:

Signalment:
2-month-old, male-intact, French bulldog, *Canis familiaris*, dog

History:
2-week history of vomiting, diarrhea, hyporexia, and lethargy. Generalized subcutaneous edema on presentation. Parvovirus snap test negative. Fecal culture:

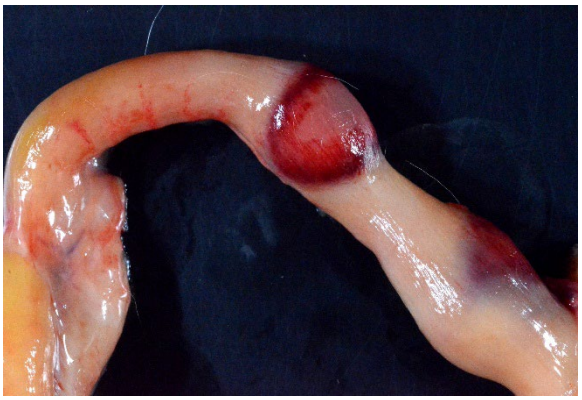

Figure 2-1: Colon, dog. The serosal surface of the distal colon contains two, 10 x 15 x 4mm, ovoid, expansile, targetoid lesions (pale pink center surrounded by a hyperemic rim). (Photograph courtesy of: University of California, Davis School of Veterinary Medicine, Anatomic Pathology service https://www.vetmed.ucdavis.edu/hospital/support-services/lab-services/anatomic-pathology-service)

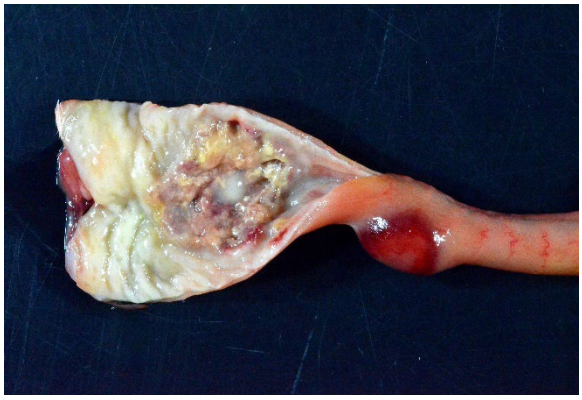

Figure 2-2: Colon, dog. The corresponding colonic mucosa of these foci is friable, thickened up to 8 mm thick, with an irregular corrugated mucosal surface that is mottled tan to brown, with a central area of pasty, white exudate. (Photograph courtesy of: University of California, Davis School of Veterinary Medicine, Anatomic Pathology service https://www.vetmed.ucdavis.edu/hospital/support-services/lab-services/anatomic-pathology-service)

negative for Salmonella sp., C. difficile, C. perfringens.

Gross Pathology:

The subcutis is diffusely expanded by up to 1 cm of gelatinous, translucent, pale yellow material (edema).

On the serosal surface of the distal colon are two, 10 x 15 x 4mm, ovoid, expansile, targetoid (pale pink center surrounded by a hyperemic rim) foci, located 15mm apart and approximately 2cm orad from the anus. The corresponding colonic mucosa of these foci is friable thickened up to 8 mm thick, with an irregular corrugated mucosal surface that is mottled tan to brown, with a central area of pasty, white exudate (pus, ulceration and necrosis).

Laboratory Results:

Parvovirus antigen SNAP test: negative (premortem

Fecal culture: negative for Salmonella sp., C. difficile, C. perfringens.

Pan-fungal PCR (through UGA) negative

Oomycete PCR (through UGA), positive for Pythium spp.

Microscopic Description:

This slide consists of three sections of segmentally ulcerated and necrotic colon and one section of less severely affected duodenum with attached pancreas. Within the colonic sections the mucosa is segmentally necrotic with loss of cellular architecture and replacement with amorphous to fibrillary eosinophilic material (fibrin, proteinaceous exudate), scattered karyorrhectic debris, and frequent 4 to 9 um wide, hyphal elements that have 1um wide, bright eosinophilic cell walls that are nonparallel, and demonstrate irregular, non-dichotomous, lateral branching and rare septation. The underlying submucosa, muscular layers, and occasionally the serosa (transmural), are infiltrated by the previously described hyphal structures, scattered karyorrhectic debris, mixed, swollen leukocytes (neutrophils, histiocytes, lymphocytes, and rare eosinophils), and extravasated erythrocytes (hemorrhage). The intestinal wall is variably necrotic, with loss of cellular detail and loss of differential staining. Medium sized arteries within the submucosa frequently contain dense mats of hyphal structures, with individual hyphae present within the vessel walls. In segments of mucosa adjacent to the completely ulcerated regions, fibrin thrombi are frequently present within lamina propria vessels. The necrotic luminal surface is lined by dense sheets of ovoid, bright eosinophilic, 5 x 5 to 5 x 8 um structures with a thin cell wall, and irregular, pale eosinophilic, internal vacuoles (zoospores), as well as loosely clustered dark basophilic, 1 to 2 um diameter, round structures (bacteria).

The section of duodenum demonstrates multifocal ulceration down to the submucosa, with replacement by fibrin and swollen leukocytes. Clusters of the previously described yeast

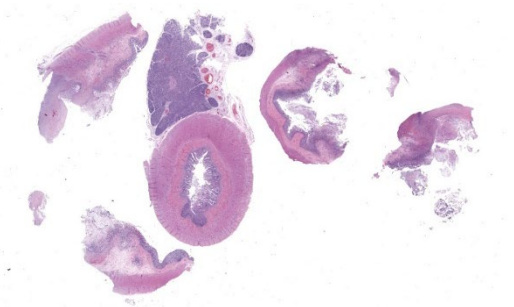

Figure 2-3: Colon, duodenum and attached pancreas, dog. Multiple ulcerated sections of colon, and an ulcerated section of duodenum with attached pancreas are submitted for examination. (HE, 10X)

structures are present within the fibrinous, luminal exudate. Villi are diffusely, markedly blunted (crypt: villous ratio ~ 1:1), fused, and the lamina propria is markedly expanded by densely packed mixed leukocytes, that include mainly lymphocytes and histiocytes, with fewer multinucleated giant cells, plasma cells, and granulocytes.

The interstitium of the pancreas is moderately to markedly expanded by dense streams of lymphocytes, plasma cells, histiocytes, and rare, fragmented neutrophils.

Contributor's Morphologic Diagnoses:

1. Colon: Fibrinonecrotizing and ulcerative, granulomatous and neutrophilic, transmural colitis, multifocal to segmental, severe, acute on chronic, with fibrin thrombi, intralesional hyphae, and intraluminal zoospores, and coccobaccili
2. Duodenum: Lymphoplasmacytic and fibrinonecrotizing duodenitis, moderate to marked, chronic, segmental with villous fusion, blunting, and intraluminal zoospores
3. Pancreas: Lymphoplasmacytic and histiocytic pancreatitis, marked, multifocal to coalescing

Contributor's Comment:

This case represents a florid case of intestinal pythiosis. The etiologic agent of pythiosis in mammals is *Pythium insidiosum*, which causes cutaneous, intestinal, and occasionally upper respiratory infections in a wide variety of species. *P. insidiosum* is an aquatic oomycete (clade Stramenopila/ heterokonts, class Oomycetes, order Pythiales, family *Pythiaceae*), with many of its closest relatives being plant pathogens that are the cause of what is colloquially known as "root rot". *Pythium* spp. are closer relatives to algae than fungi, and care should be taken to not miscategorize these organisms into the kingdom Fungi.

These water molds, unsurprisingly, preferentially grow in aquatic, warm environments. The preferable temperature range for growth ranges from 34 to 36C (93 to 97F) but growth is still possible in temperatures up to 45C (113F).[2] Historically, the distribution of this organism has been limited to tropical and subtropical environments, and in recent years (starting in 2003) increasing numbers of cases have been reported in higher latitude regions, such as Northern California and the Chincoteague national wildlife refuge in Virginia.[1,5,6] Speculation about the cause for the expansion in the geographic range of this or

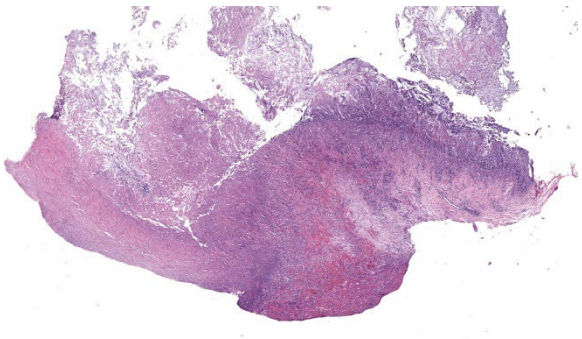

Figure 2-4: Colon, dog. Biopsy from one of the colonic lesions with full-thickness necrosis and abundant necrotic debris within the lumen (HE, 38X)

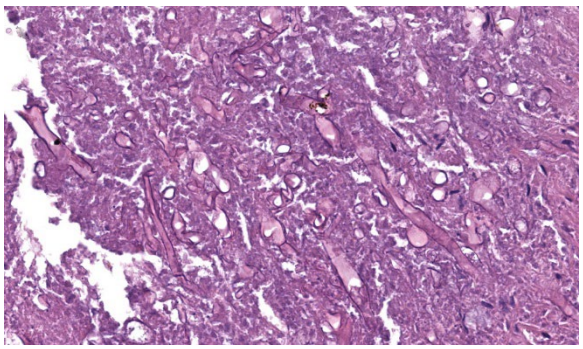

Figure 2-5: Colon, dog. The necrotic mucosa (left) contains numerous cross and tangential sections of pauciseptate 8-16um hyphae with non-parallel walls (HE, 778X)

ganism includes the adoption of environmental modifications such as rice field flooding in Northern California.[1]

Intestinal infection typically occurs through ingestion of contaminated water. Though typically not seen in tissue sections, this case included abundant intraluminal zoospores, which are the infective stage of this organism.[2] Motile zoospores are produced asexually from the bulbous sporangia formed at the terminal ends of the organism's hyphae.[4] Sexual reproduction resulting in oogonia also may occur, but the size of the intraluminal structures in this case was not consistent with oogonia, which measure 23 to 30 microns in diameter.[4] Oogonia/ oospores, unlike zoospores, can persist in sub-optimal environmental conditions and may survive for months to years.[1]

Infection of the digestive tract is the most common form of pythiosis in the dog; infections of young, large-breed dogs are most commonly reported, but have also been reported in female and small-breed dogs.[1,5] Digestive tract pythiosis has also been reported in small ruminants, and horses.[2,11] Cutaneous pythiosis occurs in dogs, horses, cats, humans, cattle, as well as a number of exotic species.[1,7] Additionally, rhinofacial pythiosis ("bullnose") has been reported in sheep in Brazil.[2]

The intestinal form of pythiosis typically involves segmental thickening with associated ulceration of any portion for the gastrointestinal tract wall, from stomach to colon with variable enlargement of associated lymph nodes.[11] Occasionally a distinct mass-like lesion composed of granulomatous and fibrous tissue will form; necrotic coagula known as "leeches" or "kunkers" can be embedded within the granulation tissue.[11] Histologically, intestinal infections consist of mural to transmural pyogranulomatous inflammation with concurrent lymphadenitis, lymphangitis, and in severe cases, peritonitis. Eosinophils, though not a prominent feature in this case, are frequently present in addition to pyogranulomatous inflammation; this is presumably due to a Th2 shifted immune response that has been associated with documented increased serum concentrations of Il-4, Il-5, and IgE.[9] In contrast to the presently discussed case, hyphal structures (as described above) are frequently difficult to discern with hematoxylin and eosin staining alone, and silver staining is often needed for visualization of the organism.[11] PAS staining is frequently poor to entirely ineffective due to lack of chitin production by the organism.[11]

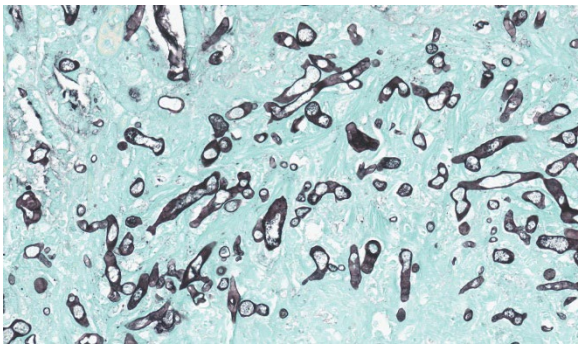

Figure 2-6: Colon, dog. A Gridley's methenamine silver bests demonstrates the morphology of the hyphae in section. (GMS, 594X)

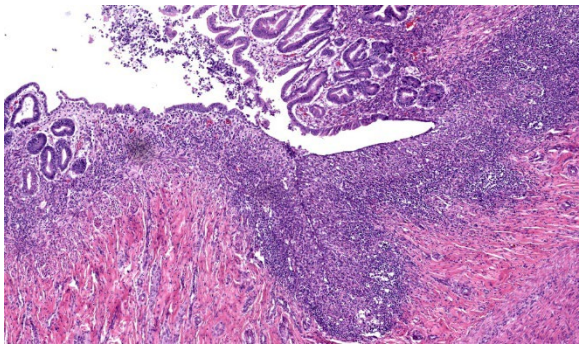

Figure 2-7: Duodenum, dog. There is a segmental duodenal ulcer extending downward into the underlying Peyer's patch. There is no evidence of fungal hyphae in this section. (HE, 124X)

The histologic lesions of intestinal pythiosis are not unique, and differential diagnoses based on histology include *Lagenidium* spp. (another oomycete), as well as a number of fungi, including zygomycetes, most notably *Conidiobolus* spp., and *Basidiobolus* spp.[2,11] Culture, serology, or molecular techniques (PCR, as used in this case) are needed for definitive diagnosis; interestingly, some panfungal PCR tests have been reported to amplify *Pythium* spp., likely due to the reliance on amplification of the internal transcribed spacer region, which is a pan-eukaryotic, non-coding segment of DNA.[8]

Unfortunately, intestinal infection with this organism can frequently be fatal. Treatment with antifungal agents is largely unsuccessful; it has been hypothesized that this may be due to the lack of ergosterol (the target of -conazole drugs) in oomycete cytoplasmic membranes.[9] Surgery to remove infected tissue is frequently the treatment of choice, and various immunotherapies have also been pursued with mixed success.[9]

Contributing Institution:
University of California, Davis School of Veterinary Medicine, Anatomic Pathology service
https://www.vetmed.ucdavis.edu/hospital/support-services/lab-services/anatomic-pathology-service

JPC Diagnoses:
1. Colon: Colitis, necrotizing and pyogranulomatous, subacute, multifocal, severe, with numerous hyphae, zoospores, and hyphal vascular invasion.
2. Duodenum: Duodenitis, ulcerative, subacute, multifocal, moderate.
3. Pancreas: Pancreatitis, lymphoplasmacytic and histiocytic, subacute, diffuse, marked, with acinar atrophy.

JPC Comment:
This was a truly phenomenal case of pythiosis and conference participants felt spoiled with how visible the hyphae and zoospores were on the slide. Oomycetes usually are much more challenging to find and tend to appear as "hyphal ghosts" from The Great Beyond, only visible with use of special paranormal photography...or a GMS stain. A classic entity, the contributor of this case provided an exceptional write-up on *Pythium insidiosum* and other major differentials in this case.

Conference discussion largely focused on a review of oomycete characteristics, most of which were covered by the contributor, as well as a few interesting facts about them that were not in the contributor's write-up. For one, infective *Pythium insidiosum* zoospores display chemotaxis towards animal hairs, intestinal mucosa, and wounded tissue. How neat is that? *Pythium* is also equipped with some impressive virulence factors that enable it to cause death and destruction regardless of it ends up in the intestinal tract or in the skin. Its cell wall components include cellulose and β-1,3-glucan. Beta-glucan, in particular, can be a target for host immune cells. [3,10] Despite

these being literal components of its own cell wall, *Pythium* comes equipped with a glucan 1,3-beta glucosidase, which breaks down β-1,3-glucan. While that may seem a bit counterintuitive, glucan 1,3-beta glucosidase acts as a virulence factor for *Pythium* by breaking down β-1,3-glucan from the cell wall, allowing the pathogen to dampen the host's immune responses and enable it to invade tissues.[3,10] This enzyme is identified as an "immunodominant" protein and is upregulated by *Pythium* during infection, suggesting it plays a key role in both disease progression and in triggering host immunity.[10]

Pythium also sports virulence factors such as has heat shock protein 70, chaperone proteins, enolase, elicitins, and urease. Much like it does in mammalian cells, heat shock protein 70 (HSP70) and other chaperone proteins protect *Pythium* from damage by binding to and stabilizing stress-induced misfolded proteins, preventing their aggregation and degradation and facilitating proper folding. HSP70 is induced under stressful conditions, such as heat (mammalian body temperature is pretty spicy if you're an oomycete), cold, infection, and inflammation. Another virulence factor, enolase, is primarily a glycolytic enzyme that catalyzes a crucial step in glycolysis to generate ATP. Enolase is also considered an immunodominant antigen.

Elicitins are proteins that are secreted by oomycetes, especially in those that infect plants, but are also seen in *Pythium insidiosum* and have dual functions. Elicitins can act as pathogen-associated molecular patterns (PAMPs) to trigger host defense responses, or they can act as virulence factors by manipulating host

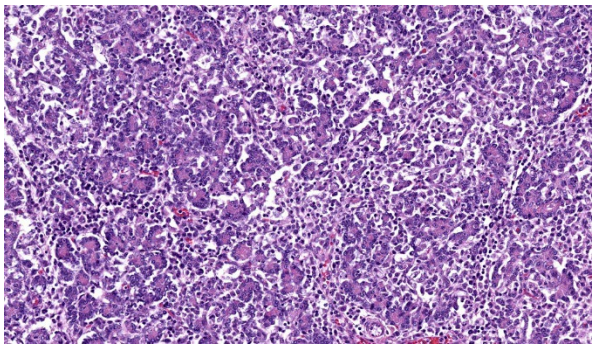

Figure 2-8: Pancreas, dog. There is marked interstitial inflammation within the pancreatic stroma by large numbers of lymphocytes and macrophages with fewer lymphocytes. There is marked atrophy of pancreatic acini. (HE, 348X).

defenses. They also act as sterol carriers, binding and transporting sterols that are essential for their growth and invasion. The dual role of elicitins makes their function context-dependent and varies based on the host and specific oomycete.

Lastly, the *P. insidiosum* urease, Ure1, hydrolyzes urea to produce nitrogen, which aids the organism's survival. Fun fact: *P. insidiosum's* urease shares similarity with the virulence factor urease, URE1, of *Cryptococcus neoformans*. In cases of pythiosis, urease is striding to the forefront as a potential diagnostic and therapeutic target because humans, as well as many domestic species, do not produce their own form of this enzyme.

References:

1. Berryessa, N., Marks, S., Pesavento, P., Krasnansky, T., Yoshimoto, S., Johnson, E. and Grooters, A.. Gastrointestinal Pythiosis in 10 Dogs from California. *Journal of Veterinary Internal Medicine*. 2008;22:1065-1069.

2. Carmo PMS, Uzal FA, Riet-Correa F. Diseases caused by *Pythium insidiosum* in sheep and goats: a review. *JVDI*. 2021;33(1):20-24.

3. Chechi JL, Franckin T, Barbosa LN, Alves FCB, Leite AL, Buzalaf MAR, Delazari Dos Santos L, Bosco SMG. Inferring putative virulence factors for *Pythium insidiosum* by proteomic approach. *Med Mycol*. 2019;57(1):92-100.

4. De Cock AW, Mendoza L, Padhye AA, Ajello L, Kaufman L. *Pythium insidiosum* sp. nov., the etiologic agent of pythiosis. *Journal of Clinical Microbiology.* 1987 Feb;25(2):344-9.

5. Fischer JR, Pace LW, Turk JR, Kreeger JM, Miller MA, Gosser HS. Gastrointestinal Pythiosis in Missouri Dogs: Eleven Cases. *JVDI*. 1994;6(3):380-382.

6. Jara M, Holcomb K, Wang X, et al. The Potential Distribution of *Pythium insidiosum* in the Chincoteague National Wildlife Refuge, Virginia. *Frontiers in Veterinary Science.* 2022;8.

7. Mauldin EA, Peters-Kennedy J. Chapter 6 - Integumentary System In: Maxie MG, ed. Jubb, Kennedy & Palmer's Pathology of Domestic Animals: Volume 1 (Sixth Edition): W.B. Saunders, 2016;509-736.

8. Meason-Smith C, Edwards EE, Older CE, et al. Panfungal Polymerase Chain Reaction for Identification of Fungal Pathogens in Formalin-Fixed Animal Tissues. *Veterinary Pathology.* 2017;54(4):640-648.

9. Mendoza L, Newton JC. Immunology and immunotherapy of the infections caused by *Pythium insidiosum*. *Med Mycol.* 2005;43(6):477-486.

10. Rujirawat T, Patumcharoenpol P, Lohnoo T, Yingyong W, Kumsang Y, Payattikul P, Tangphatsornruang S, Suriyaphol P, Reamtong O, Garg G, Kittichotirat W, Krajaejun T. Probing the phylogenomics and putative pathogenicity genes of *Pythium insidiosum* by oomycete genome analyses. *Sci Rep*. 2018;8(1):4135.

11. Uzal FA, Plattner BL, Hostetter JM. Chapter 1 - Alimentary System In: Maxie MG, ed. Jubb, Kennedy & Palmer's Pathology of Domestic Animals: Volume 2 (Sixth Edition): W.B. Saunders, 2016;1-257.e252.

CASE III:

Signalment:
14-year-old male intact Golden lion tamarin (*Leontopithecus rosalia)*

History:
The tamarin was housed in a zoo and had a chronic history (unknown duration) of waxing and waning diarrhea which was occasionally responsive to probiotics. The tamarin had a three-month history of increased symmetric dimethylarginine (SDMA) and blood urea nitrogen (BUN) that initially improved with antibiotics, but then continued to progress. Multiple renal cysts were noted on abdominal ultrasound. There was an additional two-month

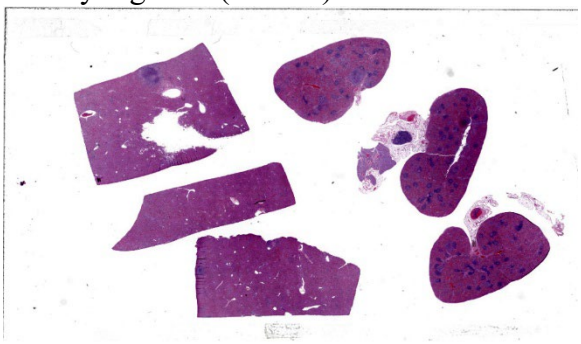

Figure 3-1: Liver and spleen, marmoset. The sections each of liver and spleen (and one section of pancreas and lymph node) are submitted for examination. AT subgross magnification, multiple foci of necrosis are visible within both the liver and splenic splenic parenchyma. (HE, 12X)

history of waxing and waning hyporexia and weight loss. Three days prior to euthanasia, the tamarin was progressively weak, lethargic, and ataxic. The tamarin was euthanized with pentobarbital following isoflurane anesthesia due to poor quality of life and prognosis.

Gross Pathology:
Approximately 20% of the hepatic and splenic parenchyma was effaced by approximately 30-40 pale tan, soft, well-demarcated foci ranging from pinpoint to 3 mm in diameter. The moderately distended gall bladder contained eight dark green choleliths ranging from 1 mm to 3 mm in diameter. Multiple lymph nodes (right mandibular, mesenteric, hepatic) were enlarged and oozed abundant pale tan purulent material on cut surface. Both kidneys had 10-15 multifocal to coalescing cystic dilations in the corticomedullary junction and medulla ranging from 2 to 5 mm in diameter. The cortex and medulla had approximately 20 multifocal punctate tan foci.

Laboratory Results:
Postmortem aerobic culture of pooled mandibular lymph node and liver grew *Listeria monocytogenes.*

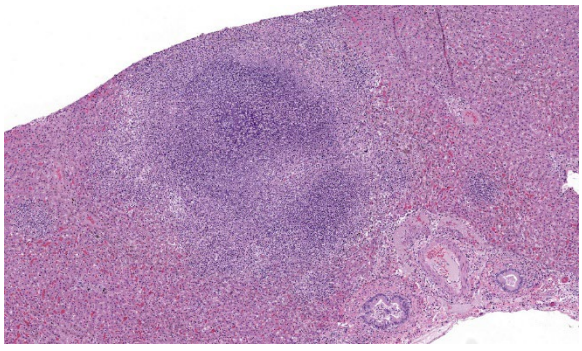

Figure 3-2: Liver, marmoset. Multiple foci of lytic necrosis ranging up to 1.5mm in diameter are scattered multifocally within the hepatic parenchyma.

Microscopic Description:
Liver: Approximately 40% of the hepatic lobular architecture is effaced by multifocal periportal to random discrete foci of lytic necrosis. Foci are composed of cellular debris, fibrin, myriad intact and fragmented neutrophils and moderate numbers of macrophages. There are small numbers of macrophages with tan to brown cytoplasmic pigment (hemosiderin vs. lipofuscin). Portal triads contain up

to four biliary duct profiles (biliary hyperplasia) and are surrounded by moderate numbers of lymphocytes, plasma cells, and macrophages. Moderate numbers of scattered hepatocytes contain brown granular cytoplasmic pigment (lipofuscin vs. hemosiderin) and cytoplasmic large discrete vacuoles. Multifocally, small hepatic vessels are partially occluded by aggregates of eosinophilic homogenous material interspersed with pyknotic debris, fragmented neutrophils, and macrophages (fibrin thrombi). Hepatic sinusoids are variably expanded with moderate numbers of erythrocytes (congestion), similar inflammatory infiltrates, and fibrin thrombi.

Spleen: Approximately 20% of the splenic parenchyma is effaced by multifocal to coalescing foci of necrosis and inflammation (similar to those described in the liver). Multifocally, the center of lymphoid follicles is hypocellular with eosinophilic karyorrhectic debris, extracellular yellow brown pigment globules (hematoidin), and moderate numbers of macrophages containing yellow brown cytoplasmic pigment (suspect hemosiderin). Splenic vessels are multifocally partially occluded by fibrin thrombi.

Contributor's Morphologic Diagnoses:
1. Liver: Moderate subacute multifocal random necrosuppurative hepatitis with periportal lymphoplasmacytic and histiocytic

cholangiohepatitis and mild biliary hyperplasia
2. Spleen: Moderate subacute multifocal necrosuppurative splenitis with lymphoid necrosis

Slides not submitted:

1. Kidney: Moderate acute multifocal suppurative nephritis, severe chronic diffuse cystic nephropathy and glomerulosclerosis with tubular proteinosis and mineralization
2. Gallbladder: Moderate cholelithiasis with mixed bacteria
3. Lymph node, mesenteric: Severe acute subacute multifocal necrosuppurative lymphadenitis

Contributor's Comment:
The combined gross findings, aerobic culture results, and histologic changes are consistent with necrotizing hepatitis, splenitis, nephritis, and lymphadenitis secondary to *Listeria monocytogenes* (sections of kidney and lymph node not included in submission). *Listeria monocytogenes* is a gram-positive, facultative anaerobic, bacillary bacterium that is abundant in soil and an opportunistic foodborne pathogen. In humans, common sources of infection include dairy products and processed fruits and vegetables. In this tamarin, contaminated fruit is postulated as the source of infection.

Infection in susceptible species can lead to various clinical syndromes, including gastroenteritis, septicemia, meningoencephalitis, abortion, and conjunctivitis. Reports of listeriosis in nonhuman primates are primarily focused on animal models of human abortion and fetal infection.[5] Spontaneous listeriosis is rarely reported.[2,6]

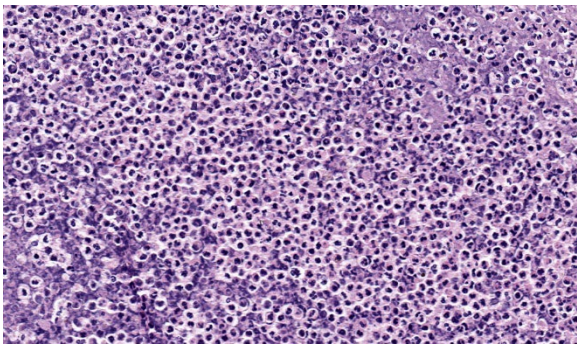

Figure 3-3: Liver, marmoset. Foci of lytic necrosis contain large numbers of viable and necrotic neutrophils admixed with fewer macrophages and abundant cellular debris. (HE, 660X)

Necrotizing hepatitis has been reported in a free-ranging Kenyan colubus monkey, and more recently, septicemic listeriosis was reported in a captive white-faced saki, which resulted in meningoencephalitis and hepatitis.[2,6] Similarly, *Listeria*-associated hepatitis is rarely reported in humans.[8] When reported in both humans and nonhuman primates, gross and histologic findings are similar to those described here. Grossly, the liver has multifocal pinpoint tan foci, which histologically correlate to multifocal areas of hepatic necrosis with infiltration of large numbers of neutrophils. Bacteria are not always histologically evident; therefore, culture is necessary for confirmatory diagnosis.[2,6,8]

As *L. monocytogenes* is an opportunistic pathogen, most infections are mild or subclinical. Multiple host risk factors contribute to severity of clinical disease. Neonates, pregnant animals, aged animals, and immunocompromised animals are most at risk for clinically significant disease. Chronic disease, including renal disease (as in this patient), liver disease, diabetes, and concurrent neoplasia all contribute to a poorer clinical presentation and prognosis.[9]

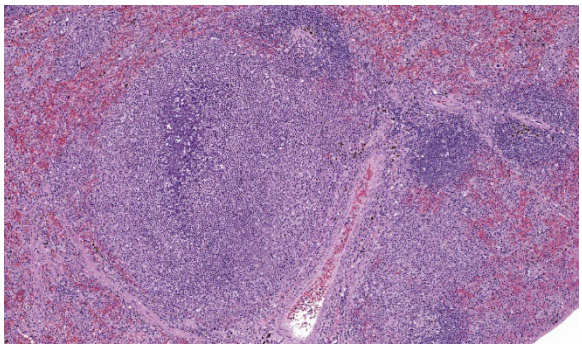

Figure 3-4: Spleen, marmoset. Similar foci of lytic necrosis ranging up to 1mm in diameter are scattered multifocally within the splenic parenchyma as well.

Infection occurs through ingestion and direct infection of enterocytes or invasion through Peyer's patches.[7] Gastroenteritis is a possible consequence of intestinal colonization, but not essential for systemic infection to occur. Rodent studies demonstrate that bacteria can cross the intestinal barrier within minutes of infection, and systemic infection can occur without histologically evident gastroenteritis.[3,4] Following intestinal infection, *L. monocytogenes* spreads to the liver through portal circulation, where it infects and proliferates within Kupffer cells and hepatocytes. In immunocompetent patients, infection is usually limited in the liver by activated macrophages and cytotoxic T-cells.[9] In acute infection, NK cells produce INF-γ, activating macrophages, which act to eliminate bacteria. In chronic infection, cytotoxic T-cells act to eliminate cells infected with *L. monocytogenes*.[1] In immunocompromised patients, infection can persist, and in some cases, become multisystemic through bacteremia and subsequent septicemia, as reported here.

Listeria monocytogenes has multiple key virulence factors involved in epithelial cell invasion (Internalin1A and Internalin1B), intracellular survival (hemolysin/lysteriolysin O), and cell-to-cell spread (ActA).[9,10] Internalin1A and Internalin 1B allows *L. monocytogenes* to infect non-phagocytic cells by interacting with lysteriolysin O to form a membrane pore through which the bacteria can enter the cell.[1,10] When engulfed by phagocytic cells, *L. monocytogenes* evades destruction by escaping the phagolysosome with listeriolysin O and phospholipases.[1,10] Once the bacteria are cytoplasmic, replication can occur. The virulence factor ActA then aids in cell-cell transfer by altering the cell cytoskeleton (actin filaments) to facilitate transfer of bacteria between cells.[1,10] In addition to aiding in phagolysosome escape, listeriolysin O and phospholipases aid in formation of bacteria-filled extracellular vesicles, which can be phagocytized by neighboring cells, leading to infection.[1,10]

Contributing Institution:
University of Wisconsin – Madison
School of Veterinary Medicine
Department of Pathobiological Sciences

JPC Diagnoses:
1. Liver: Hepatitis, necrosuppurative, acute, multifocal, moderate, with fibrin thrombi.
2. Spleen: Splenitis, necrosuppurative, acute, multifocal, moderate, with fibrin thrombi.

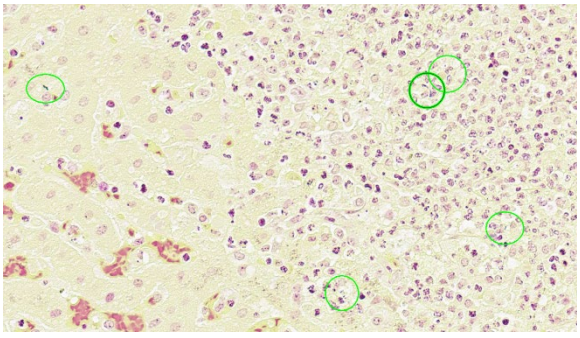

Figure 3-5.: Liver, marmoset. Rare gram-positive bacilli are present within areas of necrosis. (Brown-Brenn, 400X)

JPC Comment:

The contributor of this case wrote an excellent comment about *Listeria monocytogenes;* many topics of conference discussion focused on points from their write-up. Because the organisms were not visible without gram staining, this case proved challenging for conference participants, which some wondering about a protozoal cause for the lesions and others tentatively speculating about bacterial sepsis. Gram stains were performed in house at the JPC and revealed scattered, usually individualized, gram-positive bacilli, consistent with the *Listeria monocytogenes* identified by the contributor in this case.

Listeria monocytogenes is a resistant creature that is capable of withstanding harsh environments. It is not an organism one ever hopes to encounter in real life, but nevertheless, it occasionally finds a way to make headlines. *Listeria* is an intracellular pathogen that, as participants found, is very difficult to see on routine H&E staining. It is known to cause encephalitis and abortions but can also cause septicemia in some affected animals. It has an arsenal of virulence factors at its disposal that were nicely covered by the contributor and could make for easy boards-fodder.

LTC Cudd recounted a story about one of these virulence factors that may assist other residents in committing it to memory. She said that, during her residency, a resident-mate of hers found a video on YouTube of *Listeria monocytogenes* bacteria moving around within a cell using their ActA protein, which co-opts host cell actin to facilitate intracellular movement of the bacterium, as well as to transfer bacteria from cell to cell. The polymerized actin tails look like tiny "comets" or "rockets." In light of this, they adopted the term "Actin-A rockets" for *Listeria*. Having since watched this video, the bacteria do, in fact, look like microscopic rockets complete with fiery tails shooting around inside of the infected host cell. For educational (and entertainment) purposes alike, consider it recommended to go watch the video.

References:

1. Coelho C, Brown L, Maryam M, et al. *Listeria monocytogenes* virulence factors, including listeriolysin O, are secreted in biologically active extracellular vesicles. *J Biol Chem.* 2019;294(4):1202-1217.

2. Kock ND, Kock RA, Wambua E, et al. Listeriosis in a free-ranging colobus monkey (*Colubus guereza caudatus)* in Kenya. *The Vet Rec*. 2003:152:141-142.

3. Marco AJ, Prats N, Ramos JA, et al. A microbiological, histopathological and immunohistological study of the intragastric inoculation of *Listeria monocytogenes* in mice. *J Comp Pathol.* 1992;107(1):1-9.

4. Pron B, Boumalia C, Jaubert F, et al. Comprehensive study of the intestinal stage of listeriosis in a rat ligated ileal loop system. *Infect Immun.* 1998;66(2):747-755.

5. Schuppler M, Loessner M. The Opportunistic Pathogen *Listeria monocytogenes*: Pathogenicity and Interaction with the Mucosal Immune System. *Int J Inflam.* 2010:704321.

6. Smith MA, Takeuchi K, Brackett RE, et al. Nonhuman primate model for *Listeria monocytogenes*-induced stillbirths. *Infect Immun*. 2003;71(3):1574-1579.

7. Struthers JD, Kucerova Z, Finley A, Goe A, Huffman J, Phair K. Septicaemic Listeriosis in a White-Faced Saki (*Pithecia pithecia*). *J Comp Pathol.* 2022;194:7-13.

8. Vargas V, Alemán C, de Torres I, et al. *Listeria monocytogenes*-associated acute hepatitis in a liver transplant recipient. *Liver*. 1998;18(3):213-215.

9. Vazquez-Boland JA, Kuhn M, Berche P, et al. *Listeria* Pathogenesis and Molecular Virulence Determinants. *Clin Microbiol Rev.* 2001;14(3):584-640.

10. Zachary JF. Mechanisms of Microbial Infections. In: Zachary JF, ed. Pathologic Basis of Veterinary Disease. 7th ed. Elsevier; 2022.

CASE IV:

Signalment:
13-month-old, male, Sprague Dawley rat, *Rattus norvegicus*

History:
The animal was part of a colony of Dystrophin-deficient Sprague Dawley rats with a deletion within the exon 52 of the Dystrophin gene (R-DMDdel52 rats). These rats are used as a model for Duchenne muscular dystrophy. The rat was euthanized due to a masse on the left cheek.

Gross Pathology:
A 2-cm in diameter, well-demarcated, firm, tan mass with a central area of necrosis was observed within the left masseter muscle of the rat.

Laboratory Results:
N/A

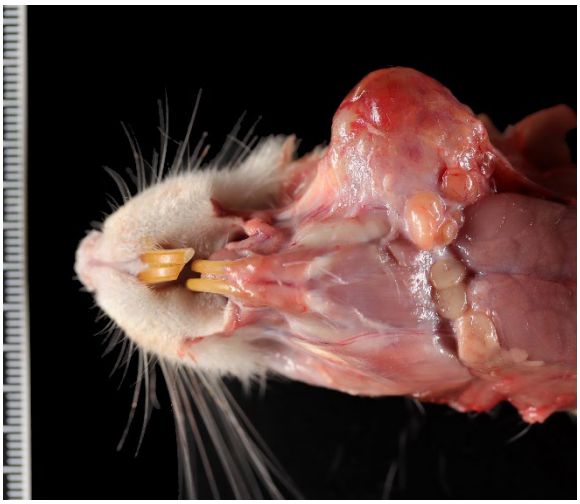

Figure 4-1: Skeletal muscle, rat. A 2-cm in diameter, well-demarcated, firm, tan mass with a central area of necrosis was observed within the left masseter muscle. (Photo courtesy of: Unité d'Histologie et d'Anatomie Pathologique, BioPôle Alfort, Département des Sciences Biologiques et Pharmaceutiques, https://www.vet-alfort.fr)

Microscopic Description:
Left masseter muscle: Expanding and replacing up to 95% of the striated muscle on the tissue section, is a well-circumscribed, unencapsulated, highly cellular and heterogeneous neoplasm. The tumor is composed of tightly packed to loosely arranged round to elongated cells, haphazardly arranged or sometimes forming streams and bundles, separated by a moderate fibrovascular stroma. Some areas have a lower cellular density with increased amount of dense fibrous stroma.

Neoplastic cells have rather distinct cell borders, a plump appearance, variable amount of an intensely eosinophilic cytoplasm, oval to elongate paracentral nuclei with finely stippled chromatin and prominent nucleoli. Round to racket-shaped or tadpod shapes cells (rhabdomyoblasts) are observed. Some cells have moreover an intensely eosinophilic appearance with a central acidophilic inclusion-like structure peripherizing the nucleus (rhabdoid cells). Numerous and scattered multinucleated giant cells are also observed.

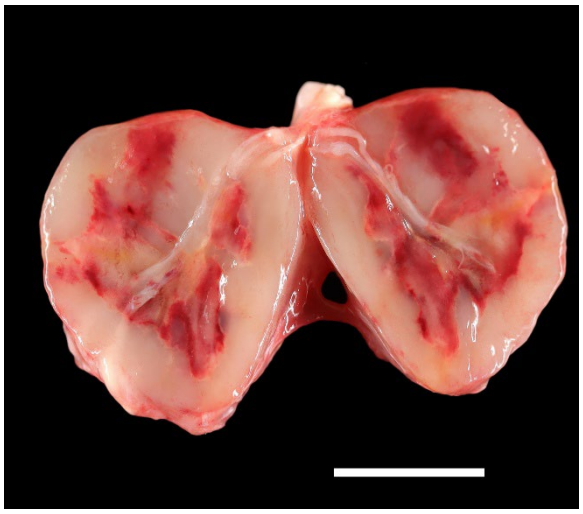

Figure 4-2: Skeletal muscle, rat. The mass from the masseter muscle, dissected and bisected. (Photo courtesy of: Unité d'Histologie et d'Anatomie Pathologique, BioPôle Alfort, Département des Sciences Biologiques et Pharmaceutiques, https://www.vet-alfort.fr)

There is marked cytologic atypia, namely anisocytosis, anisokaryosis, karyomegaly, macronucleolation, multinucleation, and bizarre mitotic figures. Mitotic figures average 10 per 10 high power fields and are often atypical.

Some preexisting dissected muscle fibers and adipocytes are present within the tumor.

Within the mass, there are several randomly distributed necrotic areas composed of eosinophilic cellular debris, viable and degenerate neutrophils. There are also lymphocytes, plasma cells and mast cells scattered among and at the periphery of the neoplasm. Surrounding tissue is compressed and neoplastic cells infiltrate the peripheral muscle fibers.

PTAH coloration was performed and showed very subtle striations in the tumor cells.

Immunohistochemistry was also performed for vimentin, myogenin and desmin. Tumor cells were strongly vimentin positive (intense cytoplasmic staining), and most cells were positive for myogenin (nuclear staining) and/or desmin (cytoplasmic staining).

Micrometastasis was observed in the associated lymph node and in the lungs (not present on slides)

Contributor's Morphologic Diagnoses:
Left masseter muscle: Rhabdomyosarcoma, pleomorphic type.

Contributor's Comment:
Rhabdomyosarcomas (RMS) are relatively rare mesenchymal neoplasms of skeletal muscle origin with varying myogenic differentiation that develop among several domestic animal species and in humans.[3,5,8,9,15] RMS can encompass a variety of gross and histologic aspects.[3] This tumor may be underdiagnosed due to these extreme variations in phenotype, age of onset, and cellular morphology that hinder diagnosis and classification.[3]

The most aggressive forms of RMS have been described in juvenile dogs younger than 2 years and include alveolar RMS and embryonal RMS.[3] Canine RMS has been described most commonly in the larynx and urogenital tract and were less frequently documented in the head, neck, and face.[3,9] Gross findings include firm, tan to white, multilobular masses with varying degrees of hemorrhage and necrosis.[3,9]

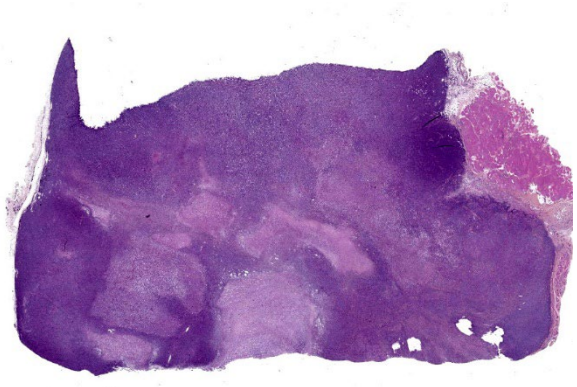

Figure 4-3: Skeletal muscle, rat. One section of the multilobular mass from the skeletal muscle is submitted for examination (normal skeletal muscle at right). (HE, 10X).

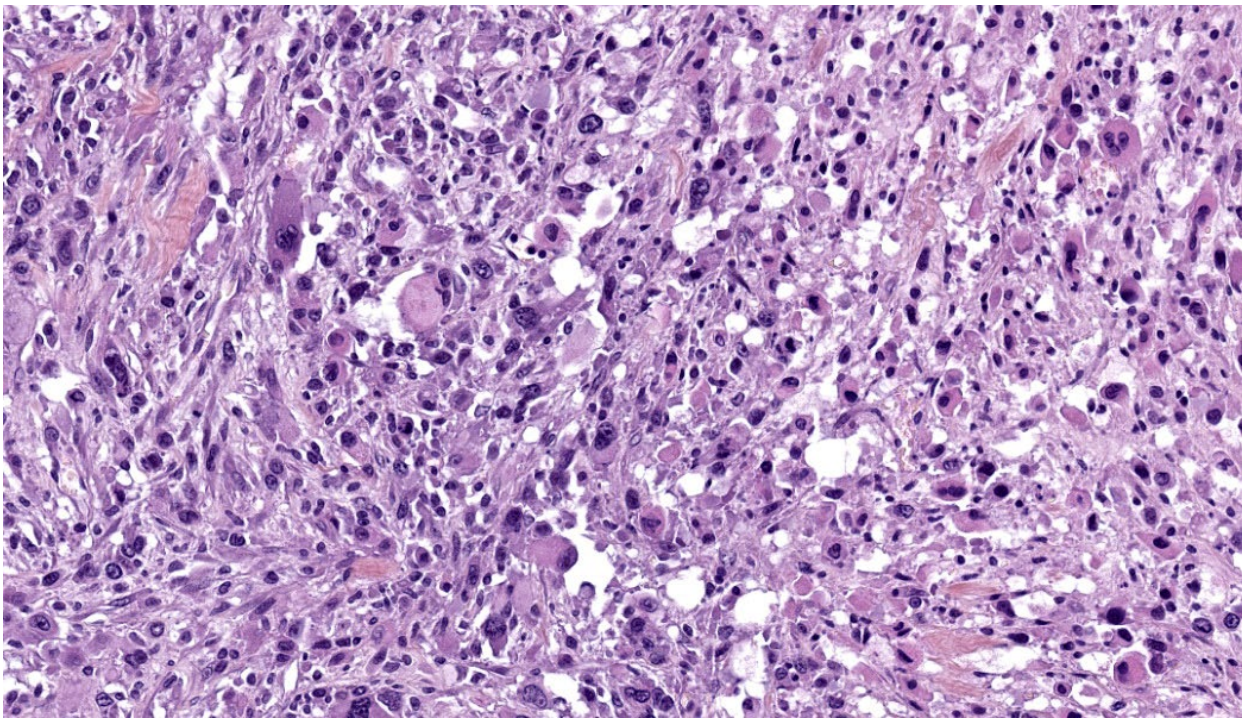

Figure 4-4: Skeletal muscle, rat. Pleomorphic polygonal to spindle cells comprise the neoplasm. (HE, 511X)

Common histologic subtypes include embryonal, botryoid, alveolar, and pleomorphic RMS.[1,3] Embryonal RMS and botryoid RMS are the most common forms in people and, seemingly, also in animals.[5,8,15]

Immunohistochemical (IHC) diagnosis of RMS in humans and dogs relies on detection of at least one muscle-specific marker (in particular, positive IHC labeling for desmin) and absence of smooth muscle markers.[1,3,14] It was recently suggested MyoD1 and myogenin should be included with desmin as part of a diagnostic IHC panel for canine RMS.[14]

Embryonal RMS is composed of either round cells or cells that exhibit different stages of development from myoblast-like and elongated cells to myotube-like ("strap") cells, that can be mononuclear or multinucleated in a myxoid stroma, with the majority of described cases arising from the head.[3,15]

Botryoid RMS is characterized by its submucosal location and its "grape-like" gross appearance. Histologically, it comprises mixed round and myotubular cells in mucinous stroma. It occurs most often in the trigone area of the urinary bladder in young large breed dogs.[3,15]

Alveolar RMS displays fibrous bands that divide small round cells into clusters and/or loose aggregates and can form thin fibrous septa.[3]

Pleomorphic RMS consists of haphazardly arranged plump spindle cells that may be admixed with scattered multinucleated cells, strap cells, racket-shaped cells, and large, round rhabdomyoblasts. Some pleomorphic RMS display cells with a rhabdoid morphology characterized by a peripherally located vesicular nucleus, prominent nucleolus, and intracytoplasmic eosinophilic hyaline

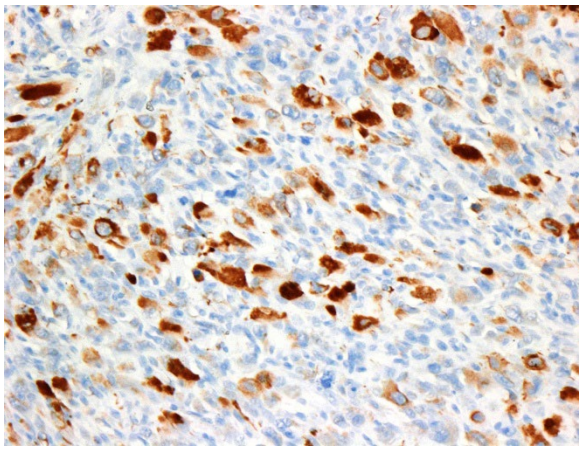

Figure 4-5: Skeletal muscle rat. Neoplastic cells demonstrate strong cytoplasmic immunopositivity for desmin. (anti-desmin, 400X) (Photo courtesy of: Unité d'Histologie et d'Anatomie Pathologique, BioPôle Alfort, Département des Sciences Biologiques et Pharmaceutiques, https://www.vet-alfort.fr)

inclusion-like structures.[5] Cells exhibit marked anisocytosis and anisokaryosis and bizarre mitotic figures.[3,15] Diagnosis of pleomorphic RMS is generally made when the whole tumor is pleomorphic, areas with embryonal or alveolar morphology are absent, and myogenic differentiation has been confirmed by immunohistochemistry.[3,15] This subclass can cause confusion since histologic evidence of skeletal muscle differentiation might not be obvious. Without immunohistochemical confirmation, such neoplasms may be diagnosed as anaplastic sarcomas.[3]

Pleomorphic rhabdomyosarcoma has been reported in dogs, cats, cows, horses, mice and rats. [2,3,4,6,9,10,13,15] It occurs less frequently than alveolar and embryonal RMS in humans. It is found more often in adult humans and animals and arises almost exclusively within skeletal muscle.[3] Noteworthy, development of pleomorphic RMS was described in a rat model of Duchenne muscular dystrophy (as in this case) following double knock-out of p16, a tumor suppressor gene, and dystrophin protein.[13]

Contributing Institution:
Ecole Nationale Veterinaire Alfort, Paris France, 7 avenue due General de Gaulle, 94700 Maisons-Alfort – 01 43 96 71 00
https://www.vet-alfort.fr

JPC Diagnoses:
Skeletal muscle: Rhabdomyosarcoma.

JPC Comment:
Although it provided a relatively straightforward diagnosis, this case stimulated great discussion in conference on subtyping of rhabdomyosarcomas, which the contributor also did an excellent job of writing about in their comment. Participants were split on what to classify this particular rhabdomyosarcoma as and, while most felt it was more likely an embryonal subtype rather than a pleomorphic due to the presence of myoblast-looking cells and strap cells, participants ultimately decided to forgo a subtype in the final morphologic diagnosis as there is currently no reported difference in clinical outcome with the different subtypes.

Other key points of conference discussion included a quick review of main sites for rhabdomyosarcoma development in other species. In dogs, these tumors often arise in the trigone of the urinary bladder, where they are usually

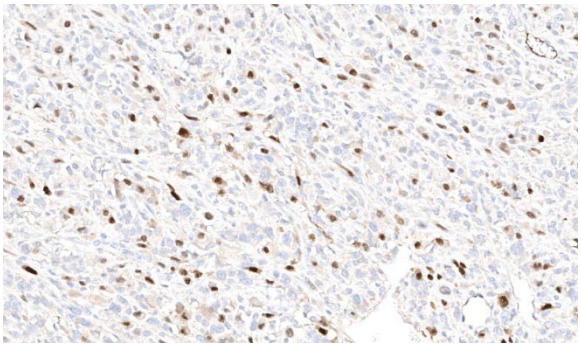

Figure 4-6: Skeletal muscle, rat. Neoplastic cells demonstrate strong regional nuclear immunoreactivity for myogenin. (anti-myogenin, 459X)

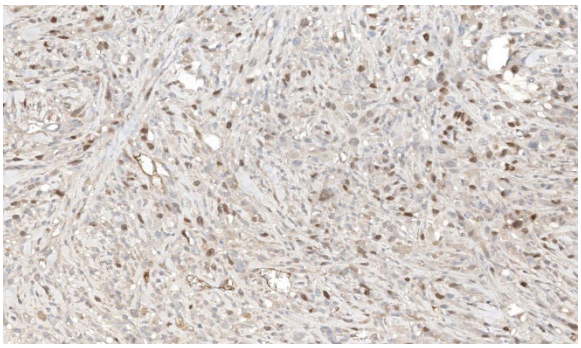

Figure 4-7: Skeletal muscle, rat. Neoplastic cells demonstrate strong regional nuclear immunoreactivity for myoD1. (anti-myoD1, 459X)

of the embryonal subtype, and in the larynx. Although rhabdomyosarcomas frequently occur in places that lack skeletal muscle (i.e. the urinary bladder), it is important to remember that they arise from myogenic precursors, which are stem cells, and stem cells can do whatever they want.

This conference case is from a dystrophin-deficient Sprague-Dawley (SD) rat, a strain of SDs used to study Duchenne muscular dystrophy of humans. Muscular dystrophy patients are predisposed to the development of rhabdomyosarcoma due to the loss of dystrophin.[7,13] Dystrophin normally functions to strengthen and stabilize muscle fibers via linking the actin cytoskeleton to the outer cell membrane and extracellular matrix. Loss of dystrophin leads to chronic damage of muscle cells and an increased rate of regeneration, which provides more chances for genetic mutations to occur.[7] Dystrophin is also a tumor suppressor gene, and its loss can result in an increased rate of not just myogenic neoplasms, but in cancer overall, especially carcinomas of the head and neck.[7]

The rhabdomyosarcoma was first described by German physician Dr. Weber in 1854 as a malignancy of striated muscle. There is some speculation on this, but he may have first described this lesion in a human tongue.[12] A more complete histologic definition was made in 1946 by Dr. Arthur Stout when he described distinct features of rhabdomyoblasts, which he stated appeared in "round, strap, racquet, and spider" shapes.[12] The current classification system for rhabdomyosarcoma was introduced in 1958 by Drs. Horn and Enterline.

Rhabdomyosarcomas are neoplasms of skeletal muscle, which is a type of striated muscle. Skeletal muscle striations are composed of alternating dark and light bands (A and I bands) that result from the highly organized, repeating arrangement of myosin and actin filaments within sarcomeres. I-bands are separated by a dark line called a Z-band, so named from the German word "zwischen" for their dark, zigzagging linear appearance. In contrast, according to Disney, "Z-bands" are "bracelets that all zombies are equipped with that send doses of electromagnetic pulses into the body, keeping the wearers from returning to their former brain-eating state. If the Z-band goes offline, the zombies revert." So, there's that.

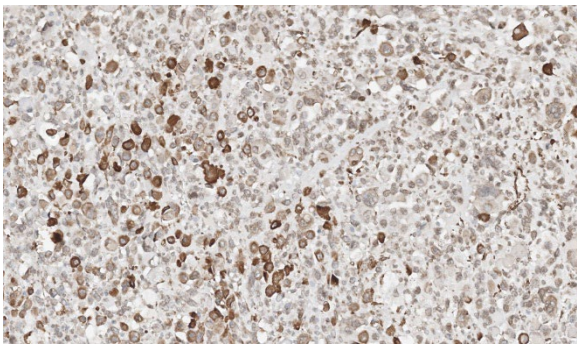

Figure 4-8: Skeletal muscle, rat. Neoplastic cells demonstrate strong regional cytoplasmic immunoreactivity for smooth muscle actin. (anti-SMA, 381X)

References:

1. Agaram NP. Evolving classification of rhabdomyosarcoma. *Histopathology*. 2022;80(1):98–108.
2. Aoyagi T, Saruta K, Asahi I, Hojo H, Shibahara T, Kadota K. Pleomorphic Rhabdomyosarcoma in a Cow. *J Vet Med Sci*. 2001;63(1):107–110.
3. Caserto BG. A Comparative Review of Canine and Human Rhabdomyosarcoma With Emphasis on Classification and Pathogenesis. *Vet Pathol*. 2013;50(5):806–826.
4. Castleman WL, Toplon DE, Clark CK, et al. Rhabdomyosarcoma in 8 Horses. *Vet Pathol*. 2011;48(6):1144–1150.
5. Goldblum JR, Folpe AL, Weiss SW. Rhabdomyosarcoma, in: Enzinger and Weiss's Soft Tissue Tumors. 2020, Mosby Elsevier, Philadelphia, PA, p. 652 696.
6. Inoue K, Yoshida M, Takahashi M, Cho Y-M, Takami S, Nishikawa A. Rhabdomyosarcoma in the Abdominal Cavity of a 12-Month-Old Female Donryu Rat. *J Toxicol Pathol*. 2009;22(3):195–197.
7. Jones L, Divakar S, Collins L, *et al.* Duchenne muscular dystrophy gene product expression is associated with survival in head and neck squamous cell carcinoma. *Sci Rep.* 2025;15:10754.
8. Meuten DJ., Cooper BJ., Valentine BA. Tumors of muscle, in: Tumors in Domestic Animals. p. 425-466. Wiley Blackwell 2017.
9. Scott EM, Teixeira LBC, Flanders DJ, Dubielzig RR, McLellan GJ. Canine orbital rhabdomyosarcoma: a report of 18 cases. *Vet Ophthalmol*. 2016;19(2):130–137.
10. Sher RB, Cox GA, Mills KD, Sundberg JP. Rhabdomyosarcomas in Aging A/J Mice. McNeil P, ed. *PLoS ONE*. 2011;6(8):e23498.
11. Spugnini EP, Filipponi M, Romani L, et al. Electrochemotherapy treatment for bilateral pleomorphic rhabdomyosarcoma in a cat. *J Small Anim Pract*. 2010;51(6):330–332.
12. Tandon A, Sethi K, Pratap Singh A. Oral rhabdomyosarcoma: A review. *J Clin Exp Dent*. 2012;4(5):e302-8.
13. Teramoto N, Ikeda M, Sugihara H, et al. Loss of p16/Ink4a drives high frequency of rhabdomyosarcoma in a rat model of Duchenne muscular dystrophy. *J Vet Med Sci*. 2021;83(9):1416–1424.
14. Tuohy JL, Byer BJ, Royer S, et al. Evaluation of Myogenin and MyoD1 as Immunohistochemical Markers of Canine Rhabdomyosarcoma. *Vet Pathol*. 2021;58(3):516–526.
15. Maxie MG, editor. Jubb, Kennedy, and Palmer's pathology of domestic animals. Elsevier 2016.